Simulation with 2+1 flavors of dynamical overlap fermions

JLQCD and TWQCD Collaborations: H. Matsufuru[*a][†] **S. Aoki,**[bc] **T. W. Chiu,**[d]
S. Hashimoto,[ae] **T. H. Hsieh,**[f] **T. Kaneko,**[ae] **J. Noaki,**[a] **K. Ogawa,**[d] **T. Onogi,**[g]
E. Shintani,[a] **N. Yamada.**[ae]

[a]*High Energy Accelerator Research Organization (KEK), Tsukuba 305-0801, Japan*

[b] *Graduate School of Pure and Applied Sciences, University of Tsukuba, Tsukuba 305-8571, Japan*

[c]*Riken BNL Research Center, Brookhaven National Laboratory, Upton, NY 11973, USA*

[d] *Physics Department, Center for Theoretical Sciences, and Center for Quantum Science and Engineering, National Taiwan University, Taipei 10617, Taiwan*

[e]*School of High Energy Accelerator Science, The Graduate University for Advanced Studies (Sokendai), Tsukuba 305-0801, Japan*

[f]*Research Center for Applied Sciences, Academia Sinica, Taipei 115, Taiwan*

[g]*Yukawa Institute for Theoretical Physics, Kyoto University, Kyoto 606-8502, Japan*

We report the status of lattice QCD simulations with 2+1 flavors of dynamical overlap fermions by the JLQCD-TWQCD Collaboration. Numerical simulations are performed on a $16^3 \times 48$ lattice at u and d quark masses ranging (1/6 -1) physical strange quark mass, and at two values of strange quark mass around the physical value. We discuss the numerical algorithms and run statistics.

The XXVI International Symposium on Lattice Field Theory
July 14 - 19, 2008
Williamsburg, Virginia, USA

---

[*]Speaker.

[†]Email: hideo.matsufuru@kek.jp.

1. Introduction

The overlap fermion [1] has a great advantage that it retains the exact chiral symmetry on the lattice [2]. This is particularly convenient in a computation of hadron masses and matrix elements, since an artificial operator mixing is forbidden and the result can be analyzed with a continuum chiral perturbation theory formulae. On the other hand, because of its high numerical cost, a systematic study with dynamical simulation is a challenging task with the present computational power.

We are performing large-scale simulations with 2 and 2+1 flavors of dynamical overlap fermions [3, 4]. As for the $N_f = 2$ simulation on a $16^3 \times 32$ lattice, the generation of configurations has been finished [5], and various physics measurements are done or in progress [3]. In this paper, we report the status of the 2+1-flavor simulation on a $16^3 \times 48$ lattice with $a \simeq 0.11$ fm and of improvement of algorithms towards simulations on larger lattices.

The next section describes our simulation setup and present status. In Section 3 we explain our attempt to accelerate the simulation by improving the solver and HMC algorithms. The last section gives summary.

2. Simulation setup and status

The overlap operator with a quark mass m is written as

$$D(m) = \left(m_0 + \frac{m}{2}\right) + \left(m_0 - \frac{m}{2}\right)\gamma_5 \text{sign}[H_W(-m_0)], \qquad (2.1)$$

where $H_W = \gamma_5 D_W$ is the hermitian Wilson-Dirac operator with a large negative mass m_0, which is set to 1.6 throughout this work. To compute the sign function of H_W, we adopt the Zolotarev rational approximation [6, 7],

$$\frac{1}{\sqrt{H_W^2}} = \frac{d_0}{\lambda_{min}}(h_W^2 + c_{2n})\sum_{l=1}^{N}\frac{b_l}{h_W^2 + c_{2l-1}}, \qquad (2.2)$$

where $h_W = H_W/\lambda_{min}$ with λ_{min} the eigenvalue having the smallest absolute value. Parameters d_0, c_l, b_l are determined depending on the condition number of H_W. The formula is valid in a region $|\lambda| \in [\lambda_{min}, \lambda_{max}]$, and its error scales as $\exp(-\lambda_{min}N)$. To keep sufficient precision while keeping N not so large, We calculate low-lying eigenvalues of H_W of $|\lambda| < \lambda_{thrs}$ so as to determine the sign function of these modes explicitly and project them out from H_W. Then λ_{thrs} replaces λ_{min} in the above formula, leading to

$$\text{sign}(H_W) = \sum_{j=1}^{N_{ev}}\text{sign}(\lambda_j)v_j \otimes v_j^\dagger + \text{sign}(H_W)P_H, \qquad (2.3)$$

where $P_H = 1 - \sum_{j=1}^{N_{ev}} v_j \otimes v_j^\dagger$, and N_{ev} the number of modes with $|\lambda_j| < \lambda_{thrs}$. The approximation formula (2.2) is applied to the second term of Eq. (2.3). In this work, we adopt $\lambda_{thrs} = 0.045$ and $N = 10$, which lead to an accuracy of $|\text{sign}^2 H_W - 1| \simeq 10^{-(7-8)}$.

For the gauge action, we use the renormalization group improved (Iwasaki) action with $\beta = 2.3$, as well as the topology fixing term. The latter is implemented with two copies extra Wilson fermions and a twisted mass ghost as [8, 9, 10]

$$\det\left(\frac{H_W^2}{H_W^2 + \mu^2}\right) = \int \mathscr{D}\chi^\dagger \mathscr{D}\chi \exp(-S_E), \tag{2.4}$$

$$S_E = \chi^\dagger \left[(D_W + i\gamma_5\mu)(D_W^\dagger D_W)^{-1}(D_W + i\gamma_5\mu)^\dagger\right]\chi. \tag{2.5}$$

Since $\lambda = 0$ is prohibited by the fermion determinant (2.4), the topological charge is fixed during the molecular-dynamics updates. This considerably decreases the simulation cost, since the overlap operator has a discontinuity at $\lambda = 0$, and when it is hit during the molecular-dynamics update one needs to treat the discontinuity using the so-called reflection/refraction prescription [11], which requires additional inversions of the overlap operator. We set the twisted ghost mass $\mu = 0.2$ throughout this work.

Dynamical simulations are performed with the hybrid Monte Carlo algorithm. In order to improve the performance of HMC, we adopt the mass preconditioning [12] together with the multi-time step procedure [13]. The molecular-dynamics step sizes are set as $\Delta\tau_{(PF2)} \gg \Delta\tau_{(PF1)} \gg \Delta\tau_{(G)} = \Delta\tau_{(E)}$, where subscripts PF2, PF1, G, and E respectively denote the preconditioned dynamical fermions, the preconditioners, the gauge field, and the extra fermion term. In this work, $\Delta\tau_{(PF2)}/\Delta\tau_{(PF1)}$ and $\Delta\tau_{(PF1)}/\Delta\tau_{(G)}$ are set to 4–6.

The one-flavor part is implemented by taking one of the chirality sectors [14], making use of the fact that $H(m)^2$ commutes with γ_5, thus

$$H^2 = P_+H^2P_+ + P_-H^2P_- \equiv Q_+ + Q_-, \qquad \det H^2 = \det Q_+ \cdot \det Q_-. \tag{2.6}$$

Except for the trivial contribution from the zero-modes, the determinant of one chirality sector gives the contribution of one flavor. Thus the pseudofermion action $S_F = \phi_\sigma^\dagger Q_\sigma^{-1}\phi_\sigma$, where σ can either be $+$ or $-$, represents the one-flavor of dynamical fermion.

The $N_f = 2+1$ simulations are performed on $16^3 \times 48$ lattices in the $Q = 0$ topological charge sector. We use 5 values of m_{ud} covering $(1/6$–$1)\, m_s^{phys}$ for each of 2 strange quark masses, $m_s = 0.08$ and 0.10, around the physical strange quark mass m_s^{phys}. At each set of parameters (m_{ud}, m_s), 2500 trajectories of a length 1 are generated after 300 trajectories for thermalization. Present performance of $m_{ud} = 0.025$ is around 2 hours for one trajectory on one rack of Blue Gene/L.

The lattice scale is set by the hadronic radius r_0 which is defined through $[r^2(\partial V(r)/\partial r)]_{r=r_0} = 1.65$, by setting the physical value $r_0 = 0.49$ fm. The static quark potential $V(r)$ is calculated with the standard procedure. Figure 1 shows the result of the lattice spacing together with the result of $N_f = 2$ simulation. The strange quark mass effect is invisibly small. A linear extrapolation gives $a(m_{ud} = 0) = 0.1075(7)$ fm for $m_s = 0.100$ and $a(m_{ud} = 0) = 0.1075(8)$ fm for $m_s = 0.080$.

3. Improvement of the algorithm

Improvement of the solver algorithm may significantly reduce the simulation cost. We have tested two algorithms; the nested CG (4DCG) method [15] and the 5-dimensional CG (5DCG) method [16], and adopt the latter in HMC in the present simulations.
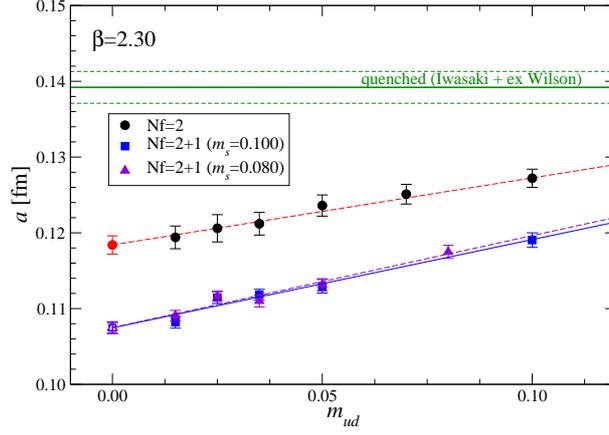
Figure 1: The lattice scale $a(r_0)$ set by $r_0 = 0.49$fm.

The 5-dimensional CG solver is based on the Schur decomposition [16] and implemented with a 5-dimensional block matrix (example with the $N = 2$ case),

$$M_5 = \begin{pmatrix} H_W & -\sqrt{q_2} & & & 0 \\ -\sqrt{q_2} & -H_W & & & \sqrt{p_2} \\ & & H_W & -\sqrt{q_1} & 0 \\ & & -\sqrt{q_1} & -H_W & \sqrt{p_1} \\ 0 & \sqrt{p_2} & 0 & \sqrt{p_1} & R\gamma_5 + p_0 H \end{pmatrix} = \left(\begin{array}{c|c} A & B \\ \hline C & D \end{array} \right). \tag{3.1}$$

Since M_5 can be decomposed as

$$M_5 = \begin{pmatrix} 1 & 0 \\ CA^{-1} & 1 \end{pmatrix} \begin{pmatrix} A & 0 \\ 0 & S \end{pmatrix} \begin{pmatrix} 1 & A^{-1}B \\ 0 & 1 \end{pmatrix}, \tag{3.2}$$

where $S = D - CA^{-1}B$, one can solve a 4D linear equation $S\psi_4 = \chi_4$ by solving a 5D equation

$$M_5 \begin{pmatrix} \phi \\ \psi_4 \end{pmatrix} = \begin{pmatrix} 0 \\ \chi_4 \end{pmatrix}. \tag{3.3}$$

Setting the parameters R, p_0, p_i and q_i ($i = 1, \ldots, N$) in Eq. (3.1) appropriately, the 5D solver can be used to invert the overlap operator approximated by Eq. (2.2). Applying the even-odd preconditioning, one needs to solve a reduced linear equation, $(1 - M_{ee}^{-1}M_{eo}M_{oo}^{-1}M_{oe})\psi_e = \chi'_e$, where even/odd blocks of M_5 is denoted by M_{ee}, M_{eo}, etc. The inversions M_{ee}^{-1} and M_{oo}^{-1} are easily calculated by forward/backward substitutions.

In $N_f = 2+1$ simulation, we implement the low-mode projection for the 5D solver [17]. The lower-right corner of Eq. 3.1 is replaced by

$$R(1 - P_H)\gamma_5(1 - P_H) + p_0 H_W + \left(m_0 + \frac{m}{2} \right) \sum_{j=1}^{N_{ev}} \text{sign}(\lambda_j) v_j \otimes v_j^\dagger, \tag{3.4}$$

While this makes the inversion of M_{ee} and M_{oo} complicated, it can be implemented with small numerical cost, because the subspace of the matrix is spanned by x_e, $\gamma_5 x_e$, v_{je}, $\gamma_5 v_{je}$ ($j = 1, \ldots, N_{ev}$).

We compare the 4D and 5D solvers on a $16^3 \times 48$ lattice, and find that the latter is faster by a factor of 3–4 in the whole region of quark mass used in this work. Thus we mainly use the 5D solver in HMC.

Besides the acceleration of the overlap solver, several acceleration techniques can be applied to the HMC, such as the chronological estimator [18], and improved integration scheme [19]. In the following, we apply the first technique to the 5D overlap solver.

The chronological estimator is a technique to accelerate the HMC update by estimating a solution of Dirac operator by making use of previous solutions at preceding MD steps [18]. Let us consider a linear equation $D[U]^\dagger D[U]\psi = b$, where U and b depend on the simulation time t. An approximate solution $\psi(t)$ may be constructed from previous solutions as

$$\psi(t) = \sum_{k=1}^{N_{pv}} c_k \psi(t - k\Delta t). \tag{3.5}$$

Two choices of c_i are tested in the following.

(1) *Polynomial extrapolation:* N_{pv}-th order polynomial extrapolation is obtained by choosing the coefficients as

$$c_k = (-)^{k-1} \frac{N_{pv}!}{k!(N_{pv} - k)!}. \tag{3.6}$$

An advantage of this method is its simplicity; one needs no additional multiplication of Dirac operator.

(2) *Minimum residual extrapolation (MRE):* c_k is determined so as to minimize

$$\Psi[\psi] = \psi^\dagger D^\dagger D\psi - b^\dagger \psi - \psi^\dagger b \tag{3.7}$$

in the subspace spanned by $\psi(t - k\Delta t)$.

To apply to the 5D solver algorithm for the overlap operator, naive way is to store the previous 5D solutions. This is memory-consuming and not feasible for simulations with large lattices. Instead, one can reconstruct the 5D solution when the corresponding 4D solution is in hand. Eq. (3.7) or (3.7) are applied to the latter. Suppose that one has a solution ψ_4 of a 4D equation, $D\psi_4 = \chi_4$. Eq. (3.3) is rewritten as

$$\begin{pmatrix} A & 0 \\ 0 & S \end{pmatrix} \begin{pmatrix} \phi + A^{-1}B\psi_4 \\ \psi_4 \end{pmatrix} = \begin{pmatrix} 0 \\ \chi_4 \end{pmatrix}. \tag{3.8}$$

Thus, when ψ_4 is already known, ϕ is given by solving $A\phi = -B\psi_4$. More explicitly,

$$\phi = \begin{pmatrix} \phi_N \\ \phi_{N-1} \\ \vdots \end{pmatrix}, \quad \phi_i = \begin{pmatrix} \sqrt{q_i} \\ H_W \end{pmatrix} \frac{\sqrt{p_i}}{H_W^2 + q_i} \psi_4, \tag{3.9}$$

which is easily calculated simultaneously by using the multishift CG solver [20].

Figure 2 shows the convergence of the 5D solver with initial guess of solution provided by the chronological estimator. We use a single configuration of the $16^3 \times 48$ lattice with $m_{ud} = 0.015$ ($m' = 0.2$) and $m_s = 0.080$ ($m' = 0.4$). Here m' denotes the mass of the preconditioner.
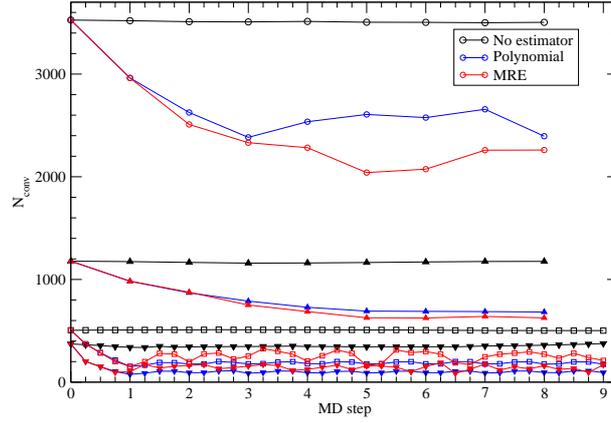
Figure 2: Convergence of the 5D solver with the chronological estimator on single configuration on $16^3 \times 48$ lattice with $m_{ud} = 0.015$ ($m' = 0.2$) and $m_s = 0.4$ ($m' = 0.4$). From top to bottom, the symbols represent numbers of iterations to achieve $|r|/|b| < 10^{-8}$ for $m_{ud} = 0.015$, $m_s = 0.08$, $m' = 0.2$ and $=0.4$, respectively.

At most 5 previous solutions are used. From top to bottom, the symbols represent numbers of iterations to achieve $|r|/|b| < 10^{-8}$ for $m_{ud} = 0.015$, $m_s = 0.08$, $m' = 0.2$ and 0.4, respectively. The chronological estimator indeed improve the convergence significantly, with both the polynomial extrapolation and MRE. Rather fluctuating behavior of MRE may be explained by the fact that we did not orthogonalize the previous vectors before applying minimization of Eq. (3.7). When two extrapolation schemes give the same level of improvement, the polynomial extrapolation is more desirable, since MRE needs additional multiplication of 4D overlap operator of $2N_{pv}$.

When one applies the chronological estimator in HMC, the tolerance must be tuned so as to keep the reversibility at a sufficient level. Therefore the gain on the performance of HMC must be carefully investigated. Such study is in progress.

Besides the chronological estimator, the construction of an approximate 5D solution (3.9) is exploited to construct an adaptive 5D solver. At an early stage of the CG iteration, one does not require the full precision to the sign function in D_{ov}. One can change the value of N_{poly} as the iteration of the solver algorithm proceeds. When one changes N_{poly}, an approximate solution at new N_{poly} is constructed from the latest 4D approximate solution. We have tested this adaptive 5D solver algorithm on our lattices, and found an improvement of about 15% in computer time.

4. Summary

We are performing a 2+1-flavor dynamical overlap simulation on a $16^3 \times 48$ lattice with $a \simeq 0.11$ fm with $Q = 0$ topological charge sector. Configuration generation has been finished, and physics measurements are in progress [21]. To perform simulations with larger lattices, further improvement of algorithms is strongly desired. In the present simulation the 5D solver with low-mode projection of H_W is adopted as the solver algorithm. We have performed exploratory study of the chronological estimator applied to the 5D solver, while practical application needs careful examination of the reversibility.

Numerical simulations are performed on Hitachi SR11000 and IBM System Blue Gene Solution at High Energy Accelerator Research Organization (KEK) under a support of its Large

References

[1] H. Neuberger, Phys. Lett. B **417** (1998) 141 [arXiv:hep-lat/9707022].

[2] M. Luscher, Phys. Lett. B **428** (1998) 342 [arXiv:hep-lat/9802011].

[3] S. Hashimoto for JLQCD and TWQCD Collaboration, these proceedings.

[4] H. Matsufuru [JLQCD Collaboration and TWQCD Collaboration], PoS **LAT2007** (2007) 018 [arXiv:0710.4225 [hep-lat]].

[5] S. Aoki *et al.* [JLQCD Collaboration], Phys. Rev. D **78** (2008) 014508 [arXiv:0803.3197 [hep-lat]].

[6] J. van den Eshof, A. Frommer, T. Lippert, K. Schilling and H. A. van der Vorst, Comput. Phys. Commun. **146** (2002) 203 [arXiv:hep-lat/0202025].

[7] T. W. Chiu, T. H. Hsieh, C. H. Huang and T. R. Huang, Phys. Rev. D **66** (2002) 114502 [arXiv:hep-lat/0206007].

[8] P. M. Vranas, arXiv:hep-lat/0001006.

[9] H. Fukaya, arXiv:hep-lat/0603008.

[10] H. Fukaya, S. Hashimoto, K. I. Ishikawa, T. Kaneko, H. Matsufuru, T. Onogi and N. Yamada [JLQCD Collaboration], Phys. Rev. D **74** (2006) 094505 [arXiv:hep-lat/0607020].

[11] Z. Fodor, S. D. Katz and K. K. Szabo, JHEP **0408** (2004) 003 [arXiv:hep-lat/0311010].

[12] M. Hasenbusch, Phys. Lett. B **519** (2001) 177 [arXiv:hep-lat/0107019].

[13] J. C. Sexton and D. H. Weingarten, Nucl. Phys. B **380** (1992) 665.

[14] A. Bode, U. M. Heller, R. G. Edwards and R. Narayanan, arXiv:hep-lat/9912043; T. DeGrand and S. Schaefer, JHEP **0607** (2006) 020 [arXiv:hep-lat/0604015].

[15] N. Cundy, J. van den Eshof, A. Frommer, S. Krieg, T. Lippert and K. Schafer, Comput. Phys. Commun. **165** (2005) 221 [arXiv:hep-lat/0405003].

[16] A. Borici, arXiv:hep-lat/0402035; R. G. Edwards, B. Joo, A. D. Kennedy, K. Orginos and U. Wenger, PoS **LAT2005** (2006) 146 [arXiv:hep-lat/0510086].

[17] S. Hashimoto *et al.* [JLQCD Collaboration], PoS (LATTICE 2007) 101.

[18] R. C. Brower, T. Ivanenko, A. R. Levi and K. N. Orginos, Nucl. Phys. B **484** (1997) 353 [arXiv:hep-lat/9509012].

[19] T. Takaishi and P. de Forcrand, Phys. Rev. E **73** (2006) 036706 [arXiv:hep-lat/0505020].

[20] A. Frommer, B. Nockel, S. Gusken, T. Lippert and K. Schilling, Int. J. Mod. Phys. C **6** (1995) 627 [arXiv:hep-lat/9504020]; B. Jegerlehner, arXiv:hep-lat/9612014.

[21] T.-W. Chiu *et al.*, [JLQCD and TWQCD Collaborations], these proceedings; .J.Noaki *et al.*, [JLQCD and TWQCD Collaborations], these proceedings.